

Oscillating laminar flow in a channel with permeable wall

Andrei Kulikovsky^{a)}

Forschungszentrum Jülich GmbH

Theory and Computation of Energy Materials (IEK-13)

Institute of Energy and Climate Research,

D-52425 Jülich, Germany^{b)}

(Dated: 25 October 2022)

Transient Navies–Stokes equations for laminar flow of incompressible fluid in a channel with permeable wall are reduced to a single equation for the transversal profile of longitudinal flow velocity. Small–amplitude harmonic perturbation of injection velocity induces oscillations of longitudinal velocity with the peak at the walls. The oscillations amplitude in peaks dramatically increases with the distance along the channel; with the frequency growth peaks come closer to the walls.

Keywords: Laminar oscillating flow in the channel, permeable wall, Berman’s model

I. INTRODUCTION

Laminar flow of incompressible fluid in channels with permeable wall(s) is of interest in ultrafiltration applications¹ and fuel cells². In 1953, Berman³ reduced 2D problem for the flow between parallel permeable walls with constant velocity of injection to a single ODE for the transversal shape of longitudinal velocity (LV) and provided an elegant asymptotic solution. Later, Berman’s approach has been used to solve the problem of a flow in pipes and ducts with permeable walls and variable along the pipe/duct velocity of suction/injection^{4–8}. So far, however, the transient effects due to time–dependent injection velocity have not been considered.

In 1929, Richardson and Tyler⁹ reported measurements of oscillating flow in a pipe with impermeable wall induced by harmonic pressure gradient. They demonstrated formation of a peak of velocity oscillations amplitude close to the pipe wall. A year later, Sexl¹⁰ developed a model for oscillating flow in a circular pipe and derived a simple solution for the radial shape of oscillating velocity amplitude. He showed that this amplitude is distributed along the radius according to the Bessel function with a peak (shoulder) positioned at the distance

$$l_* = \sqrt{\frac{\nu}{\omega}} \quad (1)$$

from the wall. Here ν is the air kinematic viscosity and ω is the angular frequency of perturbation. Harris, Peevt and Wilkinson¹¹ provided accurate measurements confirming the result of Sexl. In all these works the velocity oscillations were induced by harmonic variation of pressure gradient.

Below, unsteady laminar flow of incompressible fluid between parallel walls with the variable rate of mass injection on one of them is considered. Following the Berman’s approach, the system of transient Navier–Stokes equations is

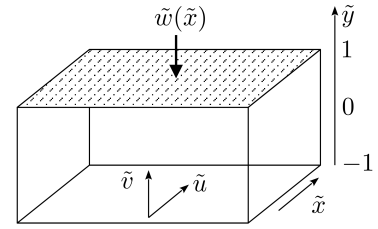


FIG. 1. Schematic of the channel. Hatched area indicates the permeable wall through which the mass enters the channel.

reduced to a single equation for the transversal shape of longitudinal flow velocity. The equation is used to study the flow response to a small–amplitude harmonic perturbation of the injection velocity. It is shown that such a perturbation induces perturbations of the longitudinal flow velocity. At high frequencies, close to the walls a peak of oscillations amplitude forms which increases dramatically with the distance along the channel. The peaks are located at the distance l_* from the wall.

II. MODEL

A. Basic equations

Consider laminar flow of incompressible fluid between parallel walls separated by the distance $2h$, with the upper wall permeable to mass injection (Figure 1). Navier–Stokes equations for u and v flow velocity components are

$$\frac{\partial u}{\partial t} + u \frac{\partial u}{\partial x} + v \frac{\partial u}{\partial y} = -\frac{1}{\rho} \frac{\partial p}{\partial x} + \nu \left(\frac{\partial^2 u}{\partial x^2} + \frac{\partial^2 u}{\partial y^2} \right) \quad (2)$$

$$\frac{\partial v}{\partial t} + u \frac{\partial v}{\partial x} + v \frac{\partial v}{\partial y} = -\frac{1}{\rho} \frac{\partial p}{\partial y} + \nu \left(\frac{\partial^2 v}{\partial x^2} + \frac{\partial^2 v}{\partial y^2} \right) \quad (3)$$

^{a)}ECS member; Electronic mail: A.Kulikovsky@fz-juelich.de

^{b)}Also at: Lomonosov Moscow State University, Research Computing Center, 119991 Moscow, Russia

Here p is the pressure and ρ is the flow density. As ρ is constant, the continuity equation is

$$\frac{\partial u}{\partial x} + \frac{\partial v}{\partial y} = 0 \quad (4)$$

Introducing dimensionless variables

$$\begin{aligned} \tilde{t} &= \frac{tu_0}{h}, & \tilde{x} &= \frac{x}{h}, & \tilde{y} &= \frac{y}{h}, & \tilde{u} &= \frac{u}{u_0}, & \tilde{v} &= \frac{v}{u_0}, \\ & & & & & & \tilde{p} &= \frac{p}{\rho u_0^2}, & \tilde{\omega} &= \frac{\omega h}{u_0}, \end{aligned} \quad (5)$$

Eqs.(2) – (4) transform to

$$\frac{\partial \tilde{u}}{\partial \tilde{t}} + \tilde{u} \frac{\partial \tilde{u}}{\partial \tilde{x}} + \tilde{v} \frac{\partial \tilde{u}}{\partial \tilde{y}} = -\frac{\partial \tilde{p}}{\partial \tilde{x}} + \frac{1}{\text{Re}} \left(\frac{\partial^2 \tilde{u}}{\partial \tilde{x}^2} + \frac{\partial^2 \tilde{u}}{\partial \tilde{y}^2} \right) \quad (6)$$

$$\frac{\partial \tilde{v}}{\partial \tilde{t}} + \tilde{u} \frac{\partial \tilde{v}}{\partial \tilde{x}} + \tilde{v} \frac{\partial \tilde{v}}{\partial \tilde{y}} = -\frac{\partial \tilde{p}}{\partial \tilde{y}} + \frac{1}{\text{Re}} \left(\frac{\partial^2 \tilde{v}}{\partial \tilde{x}^2} + \frac{\partial^2 \tilde{v}}{\partial \tilde{y}^2} \right) \quad (7)$$

$$\frac{\partial \tilde{u}}{\partial \tilde{x}} + \frac{\partial \tilde{v}}{\partial \tilde{y}} = 0, \quad (8)$$

where

$$\text{Re} = \frac{u_0 h}{\nu} \quad (9)$$

is the inlet Reynolds number and u_0 is the mean over the y -axis x -component of inlet flow velocity.

Following the idea of Berman³ we introduce a stream function

$$\psi = \left(1 + \int_0^{\tilde{x}} \tilde{\omega}(\tilde{t}, \xi) d\xi \right) f(\tilde{t}, \tilde{y}) \quad (10)$$

where $\tilde{\omega}$ is the dimensionless velocity of injection. Setting

$$\tilde{u} = \frac{\partial \psi}{\partial \tilde{y}}, \quad \tilde{v} = -\frac{\partial \psi}{\partial \tilde{x}}, \quad (11)$$

Eq.(4) is satisfied. For \tilde{u} and \tilde{v} we thus have

$$\tilde{u} = (1+R)f', \quad \tilde{v} = -\tilde{\omega}f \quad (12)$$

where

$$R \equiv \int_0^{\tilde{x}} \tilde{\omega}(\tilde{t}, \xi) d\xi \quad (13)$$

and the prime sign indicates partial derivative over \tilde{y} or \tilde{x} , depending upon the variable:

$$f' \equiv \frac{\partial f}{\partial \tilde{y}}, \quad \tilde{\omega}' \equiv \frac{\partial \tilde{\omega}}{\partial \tilde{x}}. \quad (14)$$

Substituting Eqs.(12) into Eqs.(6), (7) we come to

$$\begin{aligned} \frac{\partial(1+R)f'}{\partial \tilde{t}} + (1+R)\tilde{\omega}(f'f' - ff'') \\ = -\frac{\partial \tilde{p}}{\partial \tilde{x}} + \frac{1}{\text{Re}}(\tilde{\omega}'f' + (1+R)f''') \end{aligned} \quad (15)$$

$$\begin{aligned} -\frac{\partial(\tilde{\omega}f)}{\partial \tilde{t}} + (\tilde{\omega}^2 - (1+R)\tilde{\omega}')ff' \\ = -\frac{\partial \tilde{p}}{\partial \tilde{y}} - \frac{1}{\text{Re}}(\tilde{\omega}''f + \tilde{\omega}f'') \end{aligned} \quad (16)$$

Differentiating Eq.(15) over \tilde{y} and Eq.(16) over \tilde{x} we arrive at

$$\begin{aligned} \frac{\partial(1+R)f''}{\partial \tilde{t}} + (1+R)\tilde{\omega}(f'f'' - ff''') \\ = -\frac{\partial}{\partial \tilde{y}} \left(\frac{\partial \tilde{p}}{\partial \tilde{x}} \right) + \frac{1}{\text{Re}}(\tilde{\omega}'f'' + (1+R)f''''') \end{aligned} \quad (17)$$

$$\begin{aligned} -\frac{\partial(\tilde{\omega}'f)}{\partial \tilde{t}} + (\tilde{\omega}\tilde{\omega}' - (1+R)\tilde{\omega}'')ff' \\ = -\frac{\partial}{\partial \tilde{x}} \left(\frac{\partial \tilde{p}}{\partial \tilde{y}} \right) - \frac{1}{\text{Re}}(\tilde{\omega}'''f + \tilde{\omega}'f'') \end{aligned} \quad (18)$$

Subtracting Eq.(18) from Eq.(17) we come to

$$\begin{aligned} \frac{\partial}{\partial \tilde{t}} \left((1+R)f'' + \tilde{\omega}'f \right) \\ + (1+R)\tilde{\omega}(f'f'' - ff''') - (\tilde{\omega}\tilde{\omega}' - (1+R)\tilde{\omega}'')ff' \\ = \frac{1}{\text{Re}}(2\tilde{\omega}'f'' + (1+R)f'''' + \tilde{\omega}'''f) \end{aligned} \quad (19)$$

Eq.(19) is the general equation for the problem of a flow in channel with non-uniform along \tilde{x} and time-dependent velocity of mass injection. The boundary conditions for this equation are

$$f(1) = 1, \quad f'(1) = 0, \quad f(-1) = f'(-1) = 0 \quad (20)$$

B. Small oscillations of uniform injection velocity

It is advisable to consider the case of uniform injection velocity $\tilde{\omega}$. Setting in Eq.(19) $R = \tilde{\omega}\tilde{x}$ and chalking out the terms with $\tilde{\omega}'$, $\tilde{\omega}''$, and $\tilde{\omega}'''$, we arrive at

$$\left(\frac{\tilde{x}}{1+\tilde{x}\tilde{\omega}} \right) \frac{\partial \tilde{\omega}}{\partial \tilde{t}} f'' + \frac{\partial f''}{\partial \tilde{t}} + \tilde{\omega}(f'f'' - ff''') = \frac{f''''}{\text{Re}} \quad (21)$$

Eq.(21) can be integrated over \tilde{y} once, leading to

$$\left(\frac{\tilde{x}}{1+\tilde{x}\tilde{\omega}} \right) \frac{\partial \tilde{\omega}}{\partial \tilde{t}} f' + \frac{\partial f'}{\partial \tilde{t}} + \tilde{\omega}(f'f' - ff'') - \frac{f'''}{\text{Re}} = k \quad (22)$$

where k is determined from solution of Eq.(22) with four boundary conditions, Eq.(20). Eq.(22) is the transient version of equation derived by Berman³.

Substituting

$$\begin{aligned} \tilde{\omega} &= \tilde{\omega}_0 + \tilde{\omega}_1(\tilde{\omega}) \exp(i\tilde{\omega}\tilde{t}), \quad |\tilde{\omega}_1| \ll |\tilde{\omega}_0| \\ f &= f_0(\tilde{y}) + f_1(\tilde{\omega}, \tilde{y}) \exp(i\tilde{\omega}\tilde{t}), \quad |f_1| \ll |f_0| \\ k &= k_0 + k_1 \end{aligned} \quad (23)$$

Channel depth $2h$, m	$0.1 \cdot 10^{-2}$
Channel length L , m	1.0
Air density, ρ , kg m $^{-3}$	1.06
Air kinematic viscosity, ν , m 2 s $^{-1}$	$1.886 \cdot 10^{-5}$
Inlet flow velocity u_0 , m s $^{-1}$	10
Reynolds number Re	530
Injection velocity w , m s $^{-1}$	0.1

TABLE I. The flow parameters for the calculations.

into Eq.(22), neglecting terms with the perturbation products and subtracting the static equation Eq.(25), we come to a linear problem for the complex perturbation amplitude $f_1(\tilde{\omega}, \tilde{y})$:

$$i\tilde{\omega} \left(\frac{\tilde{x}\tilde{w}_1 f'_0}{1 + \tilde{x}\tilde{w}_0} + f'_1 \right) + \tilde{w}_0 (f_0(2f'_1 - f''_1) - f''_0 f_1) + \tilde{w}_1 (f'_0 f'_0 - f_0 f''_0) - \frac{f'''_1}{\text{Re}} = k_1 \quad (24)$$

where $f_0(\tilde{y})$ is a solution to the static Berman's equation

$$\tilde{w}_0 (f'_0 f'_0 - f_0 f''_0) - \frac{f'''_0}{\text{Re}} = k_0 \quad (25)$$

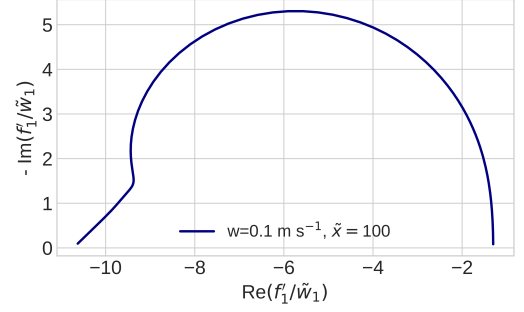
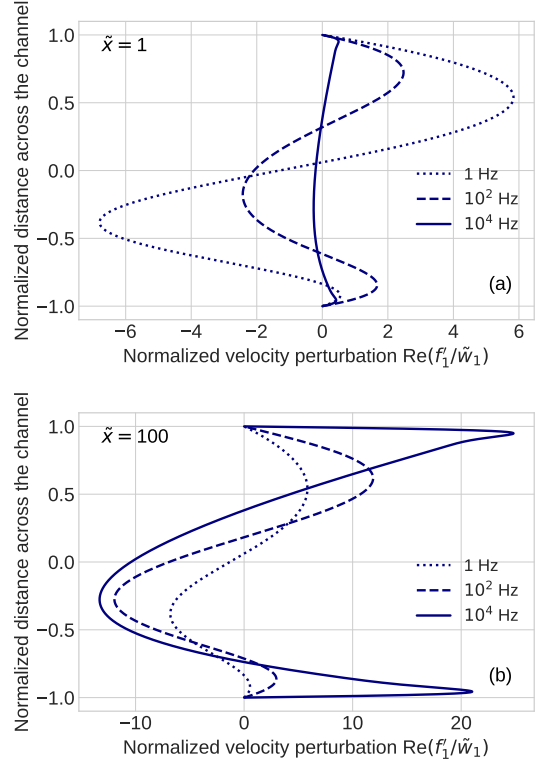
The boundary condition for f_1 at $\tilde{y} = 1$ follows from equation $\tilde{v}_0 + \tilde{v}_1 = -(\tilde{w}_0 + \tilde{w}_1)(f_0 + f_1)$. At the upper wall, $\tilde{v}_1 = -\tilde{w}_1$; neglecting the product $\tilde{w}_1 f_1$ and taking into account that $\tilde{v}_0 = -\tilde{w}_0 f_0$, $f_0(1) = 1$, we get $f_1(1) = 0$. Thus, the boundary conditions for Eq.(24) are

$$f_1(1) = f'_1(1) = f_1(-1) = f'_1(-1) = 0. \quad (26)$$

III. RESULTS AND DISCUSSION

The spectrum of f'_1 at the mid-plane $\tilde{y} = 0$ and $\tilde{x} = 100$ for the parameters in Table I resembles Warburg finite-length transport impedance¹² (Figure 2). Since $\tilde{u} \sim f'_1$, Eq.(12), of particular interest is the shape of $\text{Re}(f'_1)$ representing the LV oscillations in-phase with the applied perturbation. Eq.(24) contains a term explicitly depending on \tilde{x} ; thus, this shape changes with \tilde{x} and with the frequency. Evolution of this shape at $\tilde{x} = 1$ with the growth of frequency is depicted in Figure 3a. As can be seen, with the frequency growth, two "shoulders" at the walls and a valley between them form (the curve for 10^2 Hz, Figure 3a). The amplitude of oscillation in the valley is negative meaning that here, the oscillations decelerate the flow. Upon further frequency growth, the shoulders move toward the walls (solid line in Figure 3a). The asymmetry of the curves is due to mass injection at the upper wall.

At $\tilde{x} = 1$, the oscillations amplitude in the shoulders is on the order of unity, i.e., the relative amplitude of LV oscillations is of the same order of magnitude as the applied amplitude of injection velocity oscillations. However, LV is

FIG. 2. Nyquist spectrum of the longitudinal velocity oscillations amplitude f'_1/\tilde{w}_1 at the mid-plane $\tilde{y} = 0$ and $\tilde{x} = 100$.FIG. 3. Transversal shape of longitudinal flow velocity oscillations amplitude for the indicated frequencies at (a) $\tilde{x} = 1$ and (b) $\tilde{x} = 100$ (one tenths of the channel length).

two orders of magnitude larger than the injection velocity (Table I), meaning that the system works as a hydrodynamic "amplifier". A close analogy is field-effect transistor, in which a small variation of gate potential induces large variation of the source – drain current. With the growth of \tilde{x} , the amplitude of LV oscillations in the shoulders dramatically increases, while the oscillations amplitude in the "valley" becomes more negative (Figure 3b).

Position of the shoulders in Figure 3 can be calculated considering the problem for the flow with zero static injec-

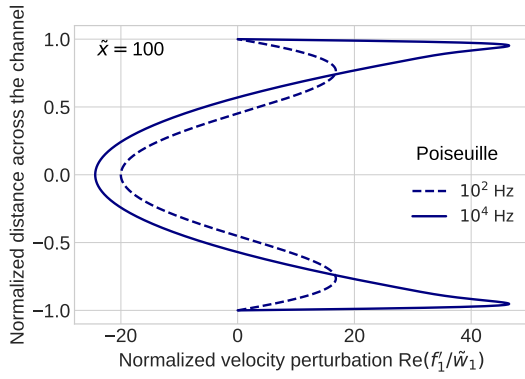


FIG. 4. Transversal shape of longitudinal flow velocity oscillations amplitude for the transient Poiseuille problem, Eq.(27).

tion velocity (Poiseuille flow), however, excited periodically at the permeable wall. An equation for the flow velocity spectrum is obtained setting $\tilde{w}_0 = 0$ in Eq.(24). Further, at large frequencies, the term $\tilde{w}_1(f'_0 f'_0 - f_0 f'_0)$ in Eq.(24) can be neglected, and we come to

$$i\tilde{\omega}(\tilde{x}\tilde{w}_1 f'_1 + f'_1) - \frac{f_1'''}{\text{Re}} = k_1 \quad (27)$$

For Poiseuille flow, $f'_0 = 3(1 - \tilde{y}^2)/4$ and solution to Eqs.(27), (26) leads to

$$f'_1 = \frac{\tilde{x}\tilde{w}_1}{4} \times \left(\frac{2i\phi \cos(\phi\tilde{y}) + \sqrt{i\tilde{\omega}\text{Re}} \cos(\phi) - 3i \sin(\phi)}{i \sin(\phi) - \sqrt{i\tilde{\omega}\text{Re}} \cos(\phi)} + 3\tilde{y}^2 \right), \quad \phi = \sqrt{-i\tilde{\omega}\text{Re}} \quad (28)$$

It is seen that the perturbation amplitude is proportional to the distance \tilde{x} . The transversal (\tilde{y} -) dependence of the perturbation amplitude for the three frequencies is shown in Figure 4. The curves are symmetric with respect to the mid-plane; nonetheless, the trend with the frequency growth is the same: a shape with the two shoulders forms (Figure 4) Interestingly, the shoulders in Figure 4 are twice larger than those in Figure 3b, i.e., zero injection velocity enhances the effect.

Asymptotic expansion of Eq.(28) for $\tilde{\omega} \rightarrow \infty$ leads to

$$\frac{f'_1}{\tilde{w}_1} = \frac{\tilde{x}}{4} \left(3\tilde{y}^2 - 1 - \frac{2i \cos(\phi\tilde{y})}{\cos(\phi)} \right), \quad \tilde{\omega} \rightarrow \infty \quad (29)$$

The term with cosines in Eq.(29) is not small only in a narrow domain near the walls. The dimensionless thickness of this domain is on the order of $1/|\phi| = 1/\sqrt{i\tilde{\omega}\text{Re}}$, which in the dimension form gives the distance between the shoulder and the wall, Eq.(1).

Finally we note that the shoulders in Figure 3 grow with \tilde{x} as long as $\tilde{x}\tilde{w}_0$ is small, as Eq.(24) shows. In long channels, for $\tilde{x}\tilde{w}_0 \gg 1$ the dependence of Eq.(24) on \tilde{x} vanishes and

the shoulders amplitude saturates. This dependence, however, retains in the general case of variable with \tilde{x} injection velocity.

IV. CONCLUSIONS

A transient model of laminar incompressible flow between parallel walls of which one is permeable to mass injection is developed. Two-dimensional transient Navier–Stokes equations and continuity equation are reduced to a single PDE for the longitudinal velocity. Linearization and Fourier–transform leads to equation for the small perturbation amplitude of this velocity.

The results show that a small perturbation of injection velocity at the permeable wall is converted to oscillations of longitudinal flow velocity. At high frequencies, the transversal profile of oscillations amplitude exhibits two peaks which dramatically increase with the distance along the channel. The peaks are located at the distance $\sqrt{\nu/\omega}$ from the walls.

- ¹G. Chao, Y. Shuili, S. Yufei, G. Zhengyang, Y. Wangzhen, and R. Liumo. A review of ultrafiltration and forward osmosis: Application and modification. *IOP Conference Series: Earth and Environmental Science*, 128:012150, Mar 2018. doi:10.1088/1755-1315/128/1/012150.
- ²M. Eikerling and A. A. Kulikovskiy. *Polymer Electrolyte Fuel Cells: Physical Principles of Materials and Operation*. CRC Press, London, 2014.
- ³A. S. Berman. Laminar flow in channels with porous walls. *J. Appl. Phys.*, 24:1232–1235, 1953. doi:10.1063/1.1721476.
- ⁴R. M. Terrill and P. W. Thomas. On laminar flow through a uniformly porous pipe. *Appl. Sci. Res.*, 21:37–67, 1969. doi:10.1007/BF00411596.
- ⁵R. M. Terrill. Laminar flow in a porous tube. *J. Fluids Eng.*, 105:303–307, 1983. doi:10.1115/1.3240992.
- ⁶A. A. Kosinski, F. P. Schmidt, and E. N. Lightfoot. Velocity profiles in porous-walled ducts. *Ind. Eng. Chem. Fundam.*, 9:502–505, 1970. doi:10.1021/i160035a033.
- ⁷J. Granger, J. Dodds, and N. Midoux. Laminar flow in channels with porous walls. *Chem. Eng. J.*, 42:193–204, 1989. doi:10.1016/0300-9467(89)80087-5.
- ⁸S. K. Karode. Laminar flow in channels with porous walls, revisited. *J. Membr. Sci.*, 191:237–241, 2001. doi:10.1016/S0376-7388(01)00546-4.
- ⁹E. G. Richardson and E. Tyler. The transverse velocity gradient near the mouths of pipes in which an alternating or continuous flow of air is established. *Proc. Phys. Soc.*, 42:1–15, 1929. doi:10.1088/0959-5309/42/1/302.
- ¹⁰T. Sexl. Über den von E. G. Richardson entdeckten Annulareffekt. *Z. Phys.*, 61:349–362, 1930. doi:10.1007/BF01340631.
- ¹¹J. Harris, G. Peevt, and W. L. Wilkinson. Velocity profiles in laminar oscillatory flow in tubes. *J. Phys. E: Sci. Instrum.*, 2:913–916, 1969. doi:10.1088/0022-3735/2/11/301.
- ¹²E. Warburg. Über das Verhalten sogenannter unpolarisierbarer Elektroden gegen Wechselstrom. *Ann. Physik und Chemie*, 67:493–499, 1899. doi:10.1002/andp.18993030302.